# Graphene-Based Micro-Rectenna

Ursula C. Resende, Thiago H. G. Mello, Gabriel A. T. Almeida, and Sandro T. M. Gonçalves
Department of Electrical Engineering, CEFET-MG, Minas Gerais 30510-000, Brazil

**The growing demand for sustainable energy generation has often pointed to solar energy as a very promising alternative. A new way to harvest solar energy is through solar rectennas. These systems are the integration of micro size antennas and nano diodes. In this way, electromagnetic energy can be captured and converted to the form of direct current. The challenges for the development of this technology are due to the submicron sizes since the theory that describes the operation of antennas moves away from classical electromagnetic behavior and incorporates quantum effects. At the same time, diodes operating in tens or hundreds of THz need specific properties. Within this context, this work presents an investigative study on solar rectennas for operation in THz range by using a bowtie antenna and a geometric diode, both based on graphene.**

***Index Terms*—Computational Modeling, Monte Carlo Simulations, Graphene, Energy Harvesting.**

## I. INTRODUCTION

THE solar energy capture utilizes well-established technologies. Some commercially available methods include photothermal generators [1] and solar cells based on the photoelectric effect, whose commercial and research-level efficiency are about $25\,\%$ and $46\,\%$, respectively, while theoretical cells consisting of an infinite number of layers can reach an efficiency limit of up to $86.8\,\%$ [2]. However, since special semiconductors compose these devices, they should be manufactured under harsh conditions that lead to relatively high prices.

As an alternative, researchers have been investigating and developing the use of optical rectennas, which are antennas coupled to rectifiers circuits operating at high frequencies, typically in the tens or hundreds of THz range [3], [4]. By interpreting solar radiation as a collection of Electromagnetic (EM) waves, micrometer-sized antennas can convert it into alternating current, while a nanometric diode handles the rectification process. Theoretically, optical rectennas can achieve an efficiency of up to $93.3\%$ [5], [6], known as the Landsberg limit, in addition to doesn't require a tracking system as they can be designed so that their incidence acceptance angle is greater than that of photovoltaic solar cells [5].

Solar energy capture using rectennas is a promising technique based on the high intensity and availability of solar radiation. However, the high frequencies associated with more energetic solar bands make this process a challenging task, primarily due to rectification, wave coherence [5], devices assemble, and simulations where quantum behavior is more notable. In light of these considerations, a methodic study at 30 THz, a lower frequency range within the infrared spectrum, yet still energetic, appears as an alternative as all bodies emit heat waves in this portion of the spectrum.

In addition to determining the operational frequency range of the devices, the selection of the conducting material is also a crucial step, as its characteristics directly influence the emergence of Surface Plasmon-Polaritons (SPPs) in the antenna and the definition of the Mean Free Path Length (MFPL) of the rectifier (and consequently the relaxation time $\tau$). So, graphene could be chosen as a substitute for noble materials like gold in the antenna due to its strong light-matter interaction [7], [8], as well as the material for the rectifier, given that graphene possesses one of the highest known MFPLs [9], high carrier mobility, good current density and carrier concentration modulated by an electric gate field [5]. Despite these favorable characteristics, graphene remains underutilized in studies of this nature.

Corresponding author: Úrsula Resende (email: resendeursula@cefetmg.br).

Based on these relatively unexplored aspects, the aim of this study is to develop a graphene-based bowtie micro-antenna for energy harvesting in the 30 THz range. Furthermore, the objective is to conceptualize and design, aided by parametric analyses of key parameters such as length, angle, and neck, a geometric nano-diode also made of graphene to optimize the rectification performance of the input signal. For the antenna, the commercial software Computer Simulation Technology (CST®) was chosen as the simulation platform, while for the diode, a Monte Carlo (MC) method was developed in Python. The proposed MC has the advantage, compared to others in the literature [4], [10], of not discretizing time into intervals $dt \ll \tau$ but considering the total $\tau$ at each step and just accounting for reflections, if any.

## II. PHYSICAL BEHAVIOUR

The physical behavior of the diode and the antenna plays a crucial role in ensuring the efficient operation of a microrectenna in the terahertz (THz) range.

### A. Micro-Antenna

In plasmonics, plasmon describes the elementary quantum excitation associated with the collective motion of valence electrons ($e^-$) at high frequency. In other words, plasmon is the quantum quasi-particle that represents the modes of charge density oscillations in a plasma [11].

In an optical medium (with electric permittivity, $\epsilon$, and/or magnetic permeability, $\mu$, differing from vacuum), the energy of the incident EM wave is shared between the oscillations of the EM fields and internal excitations of the medium. Therefore, the incident quantized particle can no longer be considered as a photon ($\gamma$) alone but rather as a coupling

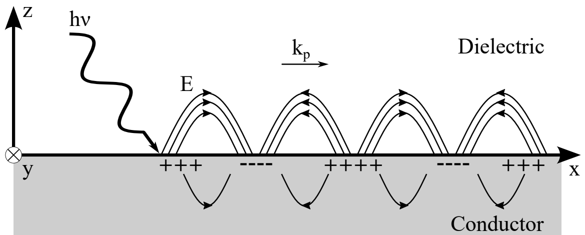


Fig. 1. SPP in the interface between a dielectric and a conductor. $k_p$ is the SPP wavevector.

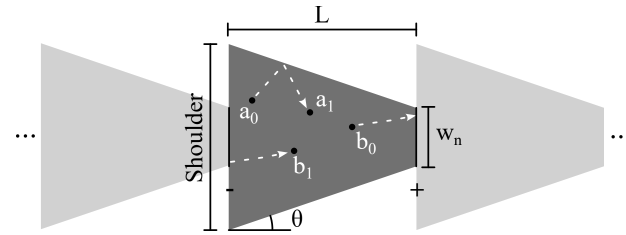


Fig. 2. Geometric diode schematic and periodicity. The default terminal polarity is defined.

between $\gamma$ and the internal degrees of freedom of the material. These operating modes are known as polaritons, and when the interaction between $\gamma$ and plasmon dominates, it gives rise to the plasmon-polariton phenomenon, or Surface Plasmon-Polariton (SPP), when happens in a thin material interfaced by a dielectric. In a thin antenna, SPPs give rise to an evanescent ordered motion on the surface of the material, resulting in an alternating current [11], [12]. A SPP wave is represented in Fig. 1. For this study, a bowtie microantenna was chosen because the electric field is concentrated in the gap between the two triangles, and it has a broader bandwidth compared to dipole and spiral antennas [5]. Additionally, the natural geometry of the bowtie antenna is suitable for connecting a rectifying device such as a diode.

### B. Geometric Diode

A geometric diode is an electronic device based on ballistic transport, where wave rectification occurs due to intentional asymmetry that defines the preferred direction of movement for free electrons. For this process to function correctly, it must be designed with dimensions on the order of the MFPL of the conductor material used [5]. Therefore, at least one of two conditions must be met: either the diode must be small, or the material must have a high MFPL. Due to the already small dimensions of the problem, graphene is considered as the conductor, which possesses a high MFPL and exhibits good conductivity [13].

Compared to other diodes commonly used, such as Metal-Insulator-Metal (MIM) diodes, the geometric diode offers several advantages. It is constructed by depositing a thin conductive layer on a dielectric, resulting in a low parasitic capacitance. This characteristic allows the geometric diode to have an RC time constant as low as $10^{-15}$ s. Additionally, due to its geometric rectification nature, the operating frequency of the geometric diode can be considerably higher compared to other rectifiers in use [13].

The mathematical modeling of the geometric diode can be approached using both quantum effects (typically employed when the dimensions are in the nanometer scale) and classical or semi-classical models such as the Drude model or the Boltzmann Transport Equation (BTE) (used when the dimensions are sufficiently large). For this work, the Drude model was chosen due to its simplicity of implementation and satisfactory results for devices in the range of hundreds of nanometers. A schematic of the diode is depicted in Fig. 2, namely arrowhead geometric diode due to it's arrow format, where $shoulder$, $L$, $\theta$, and $w_n$ are the significant performance parameters to be chosen.

## III. Simulation

### A. Monte Carlo Method

In order to simulate the behavior of the diode with various different topologies, the stochastic Monte Carlo method was chosen. Compared to other techniques such as quantum simulation, MC is advantageous because it is easy to implement, does not involve matrix inversion, and can handle any rectifier topology with proper selection of load terminals. The fact that it is a probabilistic method is not a problem as the error can be easily controlled by the setup parameters of the method.

### B. Mathematical Model

The implemented MC method considers the Drude model for $N$ agglomerated particles ($e^-$) in an electron gas [14]. In this model, the particle travels in a straight line with a constant total velocity $\vec{v}_T$ for a time interval that varies with the material, known as the relaxation time ($\tau$). $\vec{v}_T$ consists of a random component of motion (Fermi velocity $\vec{v}_F$), which also varies with the material, and a component directly related to the induced electric field vector $\vec{E}$ by the voltage between the terminals, $\tau$, and the effective mass $m_{eff}$ associated with the particles (drift velocity $\vec{v}_d$). Mathematically, it can be expressed as follows:

$$\vec{v}_T = \vec{v}_F + \vec{v}_d = \vec{v}_F + \frac{\tau N e \vec{E}}{m_{eff} N} \quad (1)$$

where $e$ is the elementary charge, the $v_d$ signal depends on the nature of the carriers, and $m_{eff}$ is defined as in [4]. After one $\tau$, if there has been no collision with the walls of the diode, it is considered that scattering has occurred. In other words, $\vec{v}_F$ takes on another random array, but with the same magnitude.

### C. Proposed Monte Carlo Algorithm

The implemented code differs from other programs found in the literature because each time step ($\Delta t$) is equal to $\tau$, rather than $\Delta t \ll \tau$. For this, it is considered that the randomly inserted particle inside the device will travel a distance $\vec{s} = \vec{s_0} + \vec{v}_T\tau$. If during this trajectory there is a collision with one or more walls of the device, the closest wall to the starting point is determined and specular reflection occurs at that point. The process is repeated for the same particle, but now with $\Delta t = \tau - t_{coll}$, where $t_{coll}$ is the time elapsed until the selected

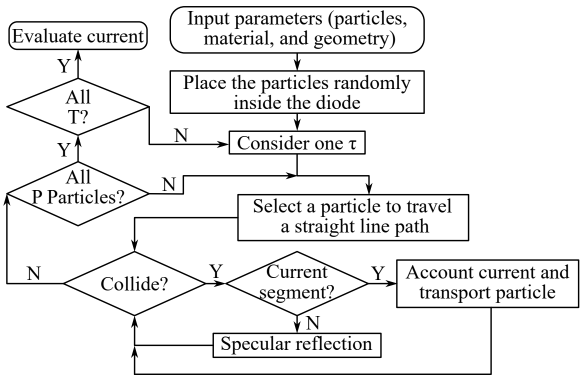


Fig. 3. Simplified flowchart for the Monte Carlo python program.

detection, as long as one $\tau$ has not elapsed. In order for the initial position of the particle not to significantly affect the rectification response, $P$ particles should be simulated until $C$ collisions, converging better as $P$ and/or $C$ increase. The current is accounted for as a relationship between the particles that cross the side corresponding to the positive terminal and the negative terminal, as shown in [4]. When a particle crosses a current counting element, it is transported to the opposite side of the voltage, but with the same $\vec{v}_T$. This occurs due to the periodic boundary condition, as represented by path $\mathrm{b}_0 \rightarrow \mathrm{b}_1$ in Fig. 2. The simplified flowchart of the program is shown in Fig. 3.

## IV. Results and Discussion

### A. Micro-antenna

Since SPPs in graphene were observed at frequencies of tens of THz, this material was used in proposed bowtie micro-antenna. The antenna components size and thickness differences make its numerical analysis very demanding, since graphene thickness ($\sim 0.34 \cdot 10^{-3}\,\mu\mathrm{m}$) is much smaller than the antenna length $2.5\,\mu\mathrm{m}$ and the incident radiation wavelength ($\lambda \sim 10.6\,\mu\mathrm{m}$), which in turn is much smaller than silicon wafer thickness ($\sim 300\,\mu\mathrm{m}$). Besides that, conductors are usually highly dispersive in the THz range, so graphene dispersive characteristics were used. Additionally, the temperature of the parameters $T = 300\,°\mathrm{C}$, chemical potential $\mu_c = 0.3\,\mathrm{eV}$ and relaxation time $\tau = 1\,\mathrm{ps}$ were selected. For the dielectric substrate, silicon dioxide and silicon models, from the CST® materials library, were considered. A Genetic Algorithm optimization was performed to obtain $S_{11} < -20\,\mathrm{dB}$ at $30\,\mathrm{THz}$. To reduce the computational demand, an electrical symmetry was considered in the $XZ$ plane and a magnetic one in the XY plane. Additionally, it was assumed open boundary conditions and solution by using Finite Integration Technique (FIT). The antenna topology is presented in Fig. 4, while $S_{11}$ for selected parameters is shown in Fig. 5. As expected, $S_{11} < -20\,\mathrm{dB}$ for a frequency closer enough to $30\,\mathrm{THz}$ with impedance of $Z_{50\,\Omega} = 54.292361 + j0.032036\,\Omega$

### B. Geometric Diode

For the diode, given the implemented stochastic method, a preliminary check of its behavior was chosen. For this purpose, a rectangle with dimensions of $1\,\mu\mathrm{m} \times 0.25\,\mu\mathrm{m}$ was simulated and compared to the theoretical analytical model of Drude [14]. The result considering $P = 100$ and $C = 10^5$ is shown in Fig. 6, where it's possible to see a good agreement between probabilistic and analytical models. Afterward, the determination of the number of particles and the number of collisions between particles and diode walls was conducted. To achieve this, a probabilistic study on the same rectangle was performed considering $10^2$ and $10^3$ distributed particles, with $10^3$, $10^4$, $10^5$, and $10^6$ collisions per voltage value. These analysis is presented in Fig. 7. All simulations considered MFPL $= 200\,\mathrm{nm}$, $v_F = 1 \times 10^6\,\mathrm{m/s}$, $T = 300\,°\mathrm{C}$, and $\epsilon = 3.9$.

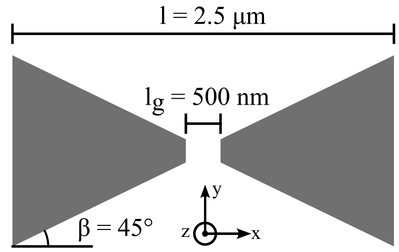


Fig. 4. Proposed antenna dimensions.

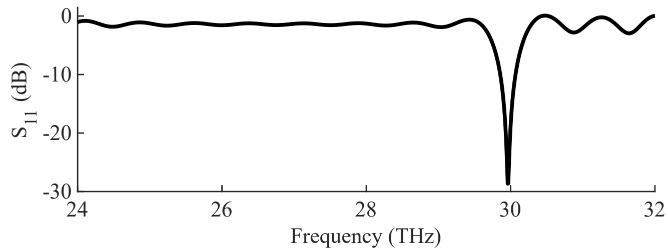


Fig. 5. $S_{11}$ for simulated micro-antenna.

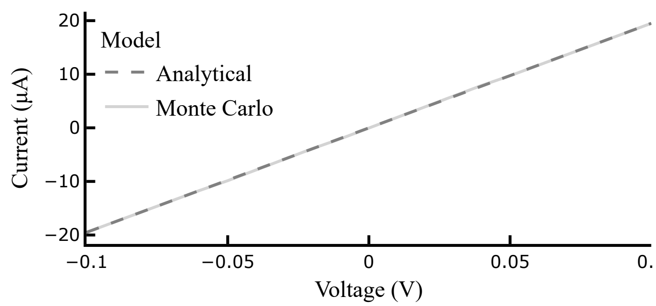


Fig. 6. Comparison between MC and Drude analytical model for a rectangle.

Based on the previous results, P was chosen as 100 particles, as the system exhibited a lower standard deviation. This is because, with more particles, a certain $C$ is reached more quickly, resulting in a significant correlation between the initial position of the particle and the calculated current. $C$ was chosen as $10^5$ based on the best trade-off between simulation accuracy and computational time.

Once the convergence parameters for the MC were defined, a parametric study of the diode was conducted, in which the geometric quantities were varied one at a time to obtain the best configuration among those studied. The first simulation

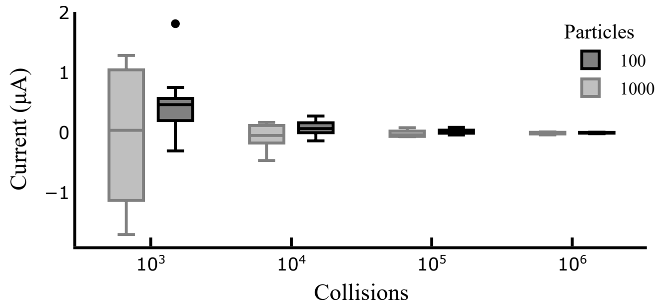


Fig. 7. Statistical MC stability analysis.

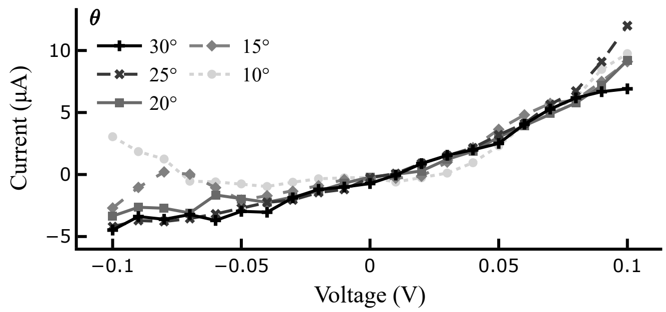


Fig. 8. Study of $\theta$ in diode behaviour.

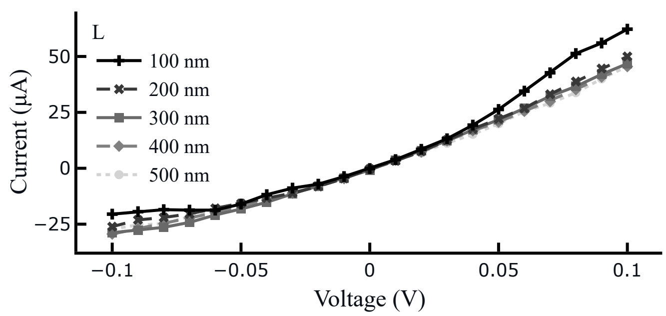


Fig. 9. Study of $L$ in diode behaviour.

corresponds to $\theta$. In this simulation, the angle was varied between $10^\circ$ and $30^\circ$, with $L = 100\,\mathrm{nm}$ and $w_n = 10\,\mathrm{nm}$. The resulting currents are shown in Fig. 8. It can be observed that for small values of theta, the diode exhibits positive currents even when a negative voltage is applied. One of the causes of this this behavior is that, in order to keep the other parameters constant, it was necessary to increase the shoulder length, which in turn enhances the reflection region of the particle only at the negative terminal while keeping it constant at the positive terminal. Since the current is a relationship between charges flowing through both terminals, a decrease in one of then alters the diode's response. Thus, the best response was obtained with $\theta = 25^\circ$.

Another study was proposed to evaluate the effect of variations in $L$. For this, a range of $100\,\mathrm{nm}$ to $500\,\mathrm{nm}$ with steps of $100\,\mathrm{nm}$ was considered, with $\theta = 15^\circ$ and $w_n = 50\,\mathrm{nm}$. The results are presented in Fig. 9. Due to the need for asymmetry for rectification, the best response is associated with $L = 100\,\mathrm{nm}$.

Lastly, we consider the effect of $w_n$ on the device. For this,

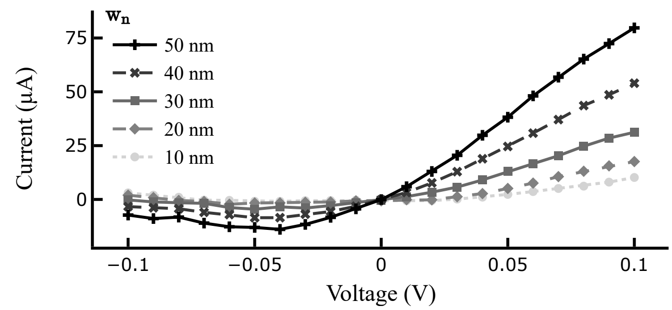


Fig. 10. Study of $w_n$ in diode behaviour.

$w_n$ was varied from $10\,\mathrm{nm}$ to $50\,\mathrm{nm}$ with steps of $10\,\mathrm{nm}$, while keeping theta and L constant at $\theta = 10^\circ$ and $100\,\mathrm{nm}$, respectively. In this case, the best response was obtained for $w_n = 50\,\mathrm{nm}$, showing considerable asymmetry and output current for positive voltages. The voltage range chosen for the simulations was between $-0.1\,\mathrm{V}$ and $0.1\,\mathrm{V}$ because, for these values, $v_d$ is considerably smaller than $v_F$, ensuring the proper functioning of the Drude model and consequently the validity of the MC method.

All the obtained results demonstrate the potential use of graphene in the composition of the micro-antenna and geometric diode, and also confirm the validity of the proposed mathematical modeling, based on the Monte Carlo method.

## Acknowledgment

This work was partially supported by FAPEMIG, CAPES, Cnpq, and CEFET-MG.

## References

[1] J. Lin, M. Lyu, and D. Shi, "3d solar harvesting and energy generation via multilayers of transparent porphyrin and iron oxide thin films," *Energies*, vol. 16, no. 7, p. 3173, 2023.
[2] A. De Vos, "Detailed balance limit of the efficiency of tandem solar cells," *J. Phys. D: Appl. Phys.*, vol. 13, no. 5, p. 839, 1980.
[3] D. Yadav, "Solar energy harvesting by carbon nanotube optical rectenna: A review," in *2020 IEEE International Symposium on Sustainable Energy, Signal Processing and Cyber Security (iSSSC)*, pp. 1–5, IEEE, 2020.
[4] J. Stearns and G. Moddel, "Simulation of z-shaped graphene geometric diodes using particle-in-cell monte carlo method in the quasi-ballistic regime," *Nanomaterials*, vol. 11, no. 9, p. 2361, 2021.
[5] G. Moddel and S. Grover, *Rectenna solar cells*, vol. 4. Springer, 2013.
[6] S. Joshi, *Performance limits of optical rectennas*. PhD thesis, University of Colorado at Boulder, 2015.
[7] Y. Li, K. Tantiwanichapan, A. K. Swan, and R. Paiella, "Graphene plasmonic devices for terahertz optoelectronics," *Nanophotonics*, vol. 9, no. 7, pp. 1901–1920, 2020.
[8] P. Gonçalves, N. Stenger, J. D. Cox, N. A. Mortensen, and S. Xiao, "Strong light–matter interactions enabled by polaritons in atomically thin materials," *Adv. Opt. Mater.*, vol. 8, no. 5, p. 1901473, 2020.
[9] G. Auton, J. Zhang, R. K. Kumar, H. Wang, X. Zhang, Q. Wang, E. Hill, and A. Song, "Graphene ballistic nano-rectifier with very high responsivity," *Nature Communications*, vol. 7, no. 1, p. 11670, 2016.
[10] Z. J. Zhu, *Graphene geometric diodes for optical rectennas*. PhD thesis, University of Colorado at Boulder, 2014.
[11] E. Le Ru and P. Etchegoin, *Principles of Surface-Enhanced Raman Spectroscopy: and related plasmonic effects*. Elsevier, 2008.
[12] L. Novotny and B. Hecht, *Principles of nano-optics*. Cambridge university press, 2012.
[13] H. Wang, G. Jayaswal, G. Deokar, J. Stearns, P. M. Costa, G. Moddel, and A. Shamim, "Cvd-grown monolayer graphene-based geometric diode for thz rectennas," *Nanomaterials*, vol. 11, no. 8, p. 1986, 2021.
[14] N. W. Ashcroft and N. D. Mermin, *Solid state physics*. Cengage Learning, 2022.